NeuroImage 46 (2009) 915–922

Contents lists available at ScienceDirect

NeuroImage

journal homepage: www.elsevier.com/locate/ynimg

Locating the functional and anatomical boundaries of human primary visual cortex

Oliver Hinds [a,*], Jonathan R. Polimeni [b], Niranjini Rajendran [b], Mukund Balasubramanian [c], Katrin Amunts [d,e], Karl Zilles [f,e], Eric L. Schwartz [c,g,h], Bruce Fischl [b,i], Christina Triantafyllou [j,b]

[a] Brain and Cognitive Sciences, Massachusetts Institute of Technology, USA
[b] Department of Radiology, MGH, Athinoula A. Martinos Center, Harvard Medical School, USA
[c] Department of Cognitive and Neural Systems, Boston University, USA
[d] Department of Psychiatry and Psychotherapy, University Hospital Aachen, Aachen University, Germany
[e] Institute of Medicine, Research Center Jülich GmbH, Germany
[f] C. and O. Vogt-Institut für Hirnforschung, Heinrich Heine Universität Düsseldorf, Germany
[g] Department of Electrical and Computer Engineering, Boston University, USA
[h] Department of Anatomy and Neurobiology, Boston University School of Medicine, USA
[i] Computer Science and Artificial Intelligence Laboratory, Massachusetts Institute of Technology, USA
[j] McGovern Institute for Brain Research, Massachusetts Institute of Technology, USA

ARTICLE INFO

Article history:
Received 5 January 2009
Revised 5 March 2009
Accepted 10 March 2009
Available online 26 March 2009

ABSTRACT

The primary visual cortex (V1) can be delineated both functionally by its topographic map of the visual field and anatomically by its distinct pattern of laminar myelination. Although it is commonly assumed that the specialized anatomy V1 exhibits corresponds in location with functionally defined V1, demonstrating this in human has not been possible thus far due to the difficulty of determining the location of V1 both functionally and anatomically in the same individual. In this study we use MRI to measure the anatomical and functional V1 boundaries in the same individual and demonstrate close agreement between them. Functional V1 location was measured by parcellating occipital cortex of 10 living humans into visual cortical areas based on the topographic map of the visual field measured using functional MRI. Anatomical V1 location was estimated for these same subjects using a surface-based probabilistic atlas derived from high-resolution structural MRI of the stria of Gennari in 10 intact *ex vivo* human hemispheres. To ensure that the atlas prediction was correct, it was validated against V1 location measured using an observer-independent cortical parcellation based on the laminar pattern of cell density in serial brain sections from 10 separate individuals. The close agreement between the independent anatomically and functionally derived V1 boundaries indicates that the whole extent of V1 can be accurately predicted based on cortical surface reconstructions computed from structural MRI scans, eliminating the need for functional localizers of V1. In addition, that the primary cortical folds predict the location of functional V1 suggests that the mechanism giving rise to V1 location is tied to the development of the cortical folds.

Introduction

The primary visual cortex (V1, Brodmann's area 17) is the first cortical area to receive visual input. The stria of Gennari – a set of heavily myelinated, horizontally projecting axons within the termination zone of lateral geniculate nucleus (LGN) input to V1 – provides an anatomical marker particular to V1 (Boyd and Matsubara, 2005). The LGN innervates V1 in an organized fashion with inputs from nearby regions in the visual field projecting to nearby regions in V1, resulting in an ordered topographic representation of the visual field in V1 (Holmes, 1917; Schwartz, 1977). The cortical image of the vertical meridian and outer edge of the visual field provides a functional definition of the V1 boundary complementary to the anatomical definition provided by the end of the stria. The correspondence between the functional and anatomical V1 boundaries has been thoroughly investigated in animal models (Otsuka and Hassler, 1962; Hubel and Wiesel, 1965), however their relationship has not been definitively established in individual human brains due to the difficulty of detecting the stria of Gennari *in vivo*.

Previous investigations comparing anatomically and functionally defined V1 have not had access to accurate estimates of the anatomical V1 boundary. Bridge et al. (2005) performed a study comparing anatomically and functionally delineated V1 where portions of the stria of Gennari were identified in high-resolution structural MRI and compared with a functional estimate of V1 location derived from standard fMRI-based visuotopic mapping techniques. While good agreement between the location of V1 was observed

* Corresponding author.
E-mail address: ohinds@mit.edu (O. Hinds).

1053-8119/$ – see front matter © 2009 Elsevier Inc. All rights reserved.
doi:10.1016/j.neuroimage.2009.03.036

between these two measurements, the high-resolution *in vivo* MRI was unable to provide a complete and accurate estimate of the anatomical V1 boundary due to the details of the MRI acquisition, which dictated the use of thick slices in order to achieve acceptable acquisition time and in-plane resolution. Wohlschlager et al. (2005) compared the intersubject variability in fMRI-defined and atlas-predicted V1 at the group level. While they observed fairly good correspondence between the anatomical and functional atlases, little can be inferred about the correspondence between these two boundary estimates in individuals based on group analyses. Here, we compare the boundary prediction with functionally-defined V1 in individual subjects, which allows an estimate of the error in boundary prediction.

Here, we demonstrate that the boundary of V1 derived from two independent methods for V1 localization shows close agreement in individual human subjects. First, we validate the accuracy of surface-based probabilistic atlas prediction of V1 location (Hinds et al., 2008) by comparing the location predicted by the atlas to the location of the V1 boundary derived from analysis of cytoarchitecture in serial sections (Amunts et al., 2000) in 10 *ex vivo* brains. Next, we employ our atlasing procedure to predict the location of anatomical V1 from standard structural MRI scans of ten *in vivo* subjects. Finally, a comparison with the functional V1 boundary measured in the same subjects using standard fMRI-based visuotopic mapping techniques reveals that the two boundaries are colocated up to error in the atlas prediction, which is low.

That the location of the anatomical boundary of V1 derived from the location of primary cortical folds via a surface-based atlas aligns with the functional V1 boundary suggests that the developmental mechanisms involved in these apparently independent systems are linked (Hinds et al., 2008). Furthermore, because there is little difference between the V1 boundary location derived via these independent methods, V1 functional localizers can be replaced with atlas-based localization, which can reduce the time required to perform fMRI experiments because only structural scans are required for localization. In addition, this method for structural localization provides an estimate of the whole extent of V1 in each subject, which is usually not possible using functional mapping due to the difficulty of spatially specific visual stimulation of the central and peripheral visual field. Finally, these results provide the most compelling evidence to date that the termination of the stria of Gennari corresponds to the location of the representation of the vertical meridian of the visual field in human.

Methods

MRI acquisition

Ten subjects were imaged using a 3 T TIM Trio MR System (Siemens Medical Solutions, Erlangen, Germany) using either a custom-built four-channel phased-array surface coil placed at the back of the head (subjects 1–4) or a 32-channel head coil (Wiggins et al., 2006). For subjects 5–10, structural scans were acquired on the same scanner using a three-dimensional T1-weighted MP-RAGE pulse sequence with a voxel size of $1\times1\times1$ mm^3, flip angle = 7°, TE = 3.48 ms, TI = 1100 ms, and TR = 2530 ms. Because the four-channel surface coil provides only partial brain coverage, subjects 1–4 underwent a separate scanning session on a 1.5 T MR system based on the Siemens Allegra. Parameters for these scans were: 1×1 mm in-plane resolution, 1.33 mm slice thickness, with TI = 1000 ms, TE = 3.31 ms, TR = 2500 ms, and a flip angle of 7°. Different coils were used because subjects 1–4 were acquired as part of a separate study (Polimeni et al., 2005).

For functional scans, the BOLD signal was measured using a single shot gradient echo, EPI pulse sequence. For subjects 1–4 these scans had parameters: TR = 2000 ms, TE = 30 ms, bandwidth = 2440 Hz and flip angle = 90°. Thirty 2.5 mm thick slices were acquired during each TR with in-plane resolution = 2.5×2.5 mm^2. Each functional run lasted 2.13 min (64 measurements). For subjects 5–10, functional scans had parameters: TR = 2000 ms, TE = 30 ms, bandwidth = 2298 Hz, flip angle = 90°, number of slices = 25, slice thickness = 2 mm (0.2 mm inter-slice gap), and in-plane resolution = 2×2 mm^2. Each functional run lasted 2.4 min (72 measurements).

Structural scans were processed using the FreeSurfer (http://surfer.nmr.mgh.harvard.edu/) software package (Dale and Sereno, 1993; Dale et al., 1999; Fischl and Dale, 2000; Fischl et al., 1999a,b, 2001, 2002, 2004) for automatic white and gray matter segmentation followed by cortical surface reconstruction. Image registration available as part of the AFNI (http://afni.nimh.nih.gov/afni) software package (Cox and Jesmanowicz, 1999) was used to motion correct the functional scans by aligning each to the first functional acquisition. The rigid-body spatial transformation aligning the functional and structural images was computed by registration of the target for motion correction to the whole-brain structural scan using the *autoreg-sess* tool provided as part of the FSFAST software package (http://surfer.nmr.mgh.harvard.edu/fswiki/FsFast). Errors in EPI to T1 registration were corrected manually using standard visualization and transformation techniques provided by FreeSurfer. Careful manual editing of registrations is required to achieve a projection of functional timeseries onto the cortical surface (described below) that preserves spatial information from the functional acquisitions. This process is necessarily observer-dependent because automatic, accurate, and reliable cross-modality image registration of partial brain data is an open problem. No spatial smoothing was applied to the functional images.

Measuring the V1 boundary functionally

Functional scans were performed to map the V1 boundary using the phase-encoded stimulus method of Sereno et al. (1995). During each functional run the subject was presented with one of four visual stimuli: a clockwise rotating wedge, a counterclockwise rotating wedge, an expanding ring, or a contracting ring. The wedge stimuli occupied a constant 20° of visual angle, while the rings were 0.15° wide at the minimum eccentricity of about 0.2° and expanded exponentially. The leading edge of the ring stimuli completely left the display before the leading edge appeared at the opposite stimulus edge to alleviate well-known "wrap-around" effects with these phase encoded stimuli (Duncan and Boynton, 2003; Polimeni et al., 2005).

All stimuli repeated with a period of 32 s and were filled with a thresholded white-noise pattern that was scaled with eccentricity to match cortical magnification (Daniel and Whitteridge, 1961; Schwartz, 1977; Polimeni et al., 2005). The motion of each stimulus is such that voxels sampling a particular region of the visual field will be encoded with a characteristic phase of the periodic stimulus.

Analysis of functional data was performed using the FSFAST software package. First the stimuli of the same type (rings or wedges) but of opposite direction were combined by reversing negative polarity stimuli and averaging all of the runs of a common stimulus type. Next the preferred stimulus phase at each voxel was estimated via a Fourier transform of the voxel time-course and extraction of the phase at the stimulus frequency for the ring and wedge stimuli independently. From this preferred phase a preferred eccentricity and azimuth were computed by transforming the stimulus phase into a visual field location. This preferred visual field representation was projected from the functional volume onto the subject's cortical surface, which allowed an estimate of the Jacobian matrix of the visual field coordinates along the surface of cortex. The sign of the determinant of this Jacobian matrix indicates the handedness of the coordinate system of the visual field representation, which differs between V1 and V2. Transitions in coordinate system handedness were identified manually on the cortical surface as the boundary of functionally defined V1 (Sereno et al., 1995).

Predicting the V1 boundary anatomically

Hinds et al. (2008) presented a method for predicting the location of anatomical V1 using surface-based intersubject registration of the primary cortical folds based on the method of Fischl et al. (1999b). In that study V1 location was determined via high-resolution MRI of the stria of Gennari in *ex vivo* human hemispheres. Low variability of V1 location was demonstrated in the hemispheres used to build the atlas. Here we extend this work by testing the accuracy of atlas prediction against an independent set of hemispheres for which the location of the stria of Gennari is available on a surface representation of the cortex.

Ten whole brain samples were embedded in paraffin and sectioned at 20 μm, then stained for cell bodies using the Nissl method, and digitally scanned as described previously (Roland et al., 1994). The inner and outer boundaries of gray matter were manually traced, then laminar profiles were algorithmically extracted, which allowed automatic spatial clustering of profiles to reveal the anatomical boundary of V1 (Roland et al., 1997; Amunts et al., 2000) in the serial sections. Before sectioning the brains were imaged using T1-weighted structural MRI at 1.5 T and 1 mm isotropic voxels. Registration of the histological sections to the MRI allowed projection of V1 onto surface reconstructions of the gray and white matter boundary (Fischl et al., 2008).

Each of the twenty cortical surfaces (ten left and ten right hemispheres) was registered to the surface-based atlas of Hinds et al. (2008), yielding a probability of belonging to V1 for each vertex in the surface. In a previous study this atlas was constructed using cortical surface-based intersubject registration of V1 from 20 humans where an accurate measurement of V1 was available from high-resolution structural MRI performed on intact *ex vivo* hemispheres via detection of the entire stria of Gennari. Using the known anatomical V1 boundary derived from histology, we determined the atlas probability threshold that provides a V1 boundary prediction with minimum bias. V1 boundary predictions were derived for probability thresholds from $p = 0.1$ to $p = 1.0$ in steps of 0.1, and each boundary prediction was compared to the measured V1 boundary by measuring the surface-based exact shortest-path distance (Balasubramanian et al., in press) between the boundaries at every point of the predicted boundary. This shortest-path distance was converted into a *signed*

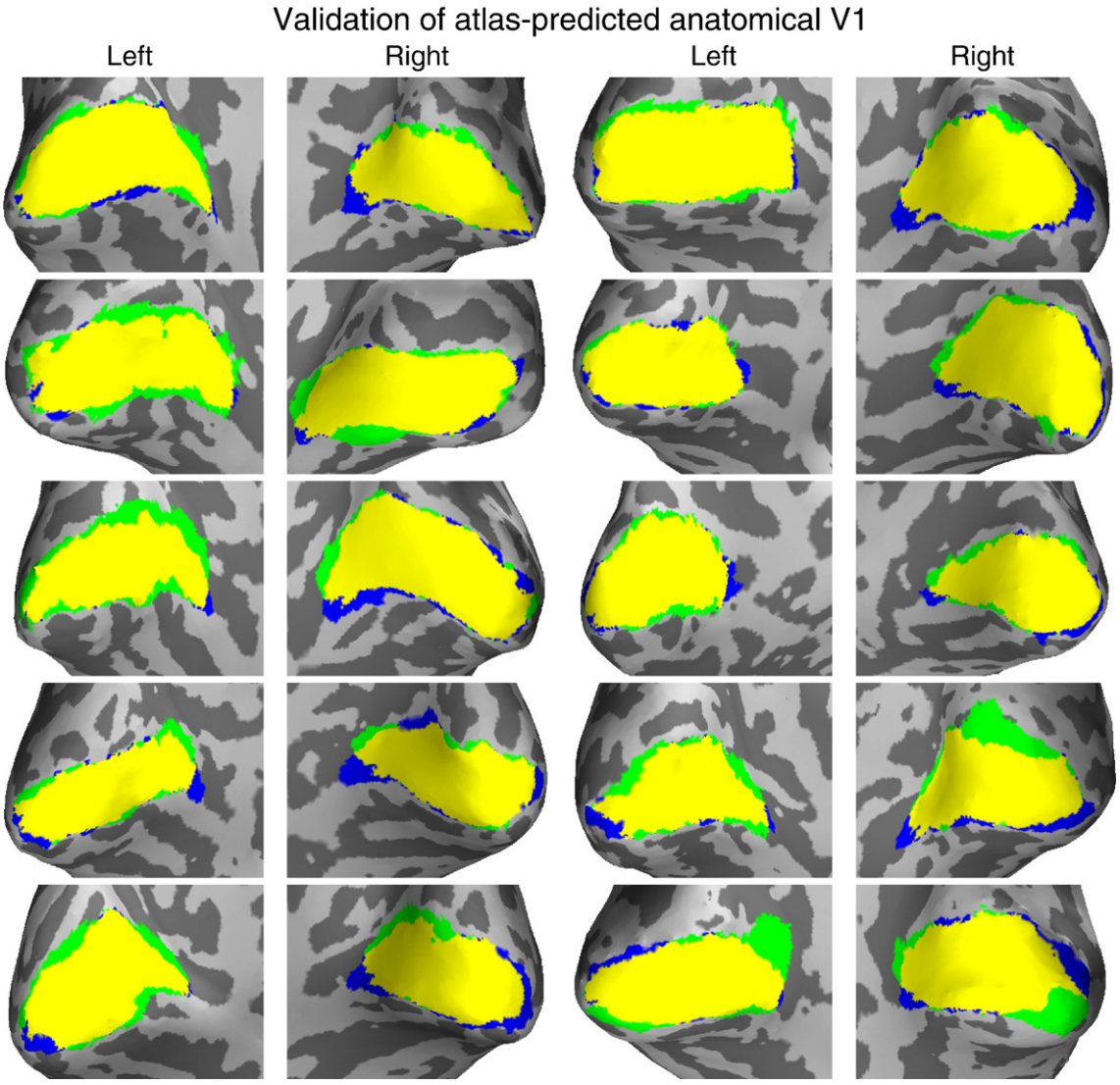

Fig. 1. Validation of the surface-based probabilistic atlas of V1 on an independent dataset. An inflated representation of both the left and right hemispheres of each subject is shown. Surfaces were reconstructed from data used by Amunts et al. (2000) to study the variability of V1 in stereotaxic space. The location of anatomical V1 determined from histology is shown in blue, the location of V1 predicted using the probabilistic atlas of Hinds et al. (2008) thresholded at $p = 0.8$ is shown in green, and the region they share is colored in yellow. Close agreement between the atlas prediction and measured location is apparent.

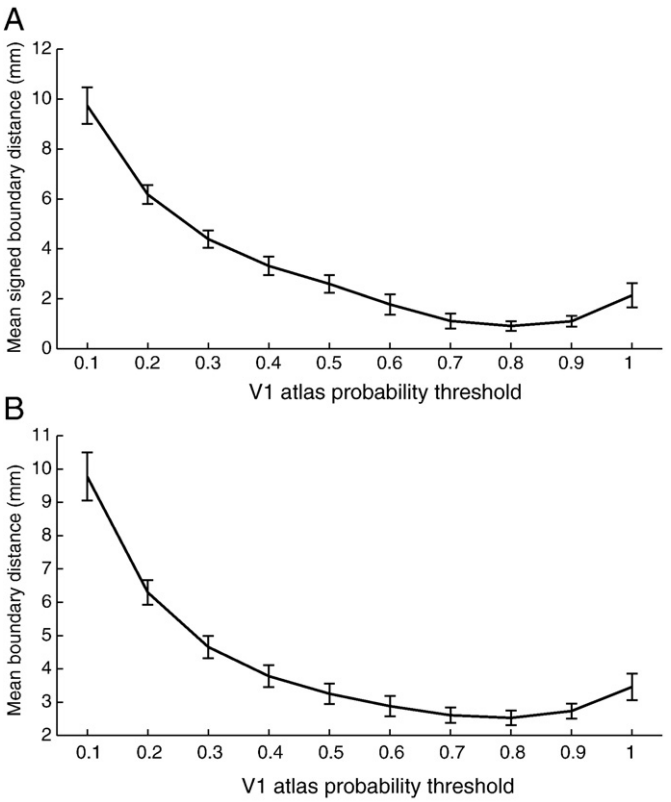

Fig. 2. Computing the atlas probability threshold that yields the minimum-bias estimate of the V1 boundary. (A) The mean signed boundary distance between the measured (from histology) and atlas-predicted V1 boundary, measured at atlas probabilities ranging from 0.1 to 1.0. The signed distance treats distances as negative if the predicted boundary is *within* the measured boundary and positive if outside. The minimum at 0.8 indicates that thresholding the probabilistic atlas at this level yields the minimum-bias V1 boundary prediction. (B) The mean unsigned boundary distance, which represents the more standard root-mean-square error between the boundary estimates.

distance by negating distances between pairs of vertices where the atlas predicted boundary vertex is inside measured V1. Signed distance is purposefully asymmetric because measured V1 is assumed to represent ground truth, and minimization of the deviation of the atlas prediction from this ground truth is desired. The V1 boundary error for a given probability threshold was computed by summing the signed distance between the measured and predicted boundaries in each individual for that threshold, then computing the mean of the absolute value of the signed distance across individuals. The probability threshold that produced the minimum-bias boundary estimate was taken to be that with minimum error.

Although the optimal probability threshold was derived from signed distances, in this study standard root-mean-square error measures are always reported as the actual distance between boundaries.

Comparing the functional and anatomical V1 boundaries

The minimum-bias atlasing procedure was used to predict the location of anatomically-defined V1 for each of the subjects with functional V1 measurements. The agreement between the anatomical and functional V1 boundaries was measured by computing the surface-based exact shortest-path distance between the two boundaries for each vertex on the functional V1 boundary. Note that because only a portion of the V1 boundary can be measured using fMRI (due to the limited amount of the visual field that can be stimulated in the MRI scanner), only the portions of V1 that represent the central 10° radius of visual field can be compared.

Results

Validation of the anatomical V1 boundary estimate

We validated that the prediction of the anatomical boundary of V1 given by the surface-based probabilistic atlas of Hinds et al. (2008) agrees with the V1 boundary location derived from histology (Amunts et al., 2000) in ten left and ten right *ex vivo* hemispheres. A comparison of the predicted and measured V1 boundary location in each of these hemispheres is shown in Fig. 1. Over all twenty hemispheres, the distance between the predicted and measured boundary was just 2.5 ± 0.03 mm (mean $\pm$ standard error). The error for the left hemispheres was 2.3 ± 0.03 mm and the error for the right hemispheres was 2.7 ± 0.04 mm. Fig. 5A shows a histogram of the distance between these two boundary estimates over all subjects and hemispheres.

To compare the atlas prediction with the measured boundary location it was necessary to threshold the atlas probabilities to derive a binary V1 label. Probabilities between 0.1 and 1.0 were tested and we found that a probability threshold of $p = 0.8$ yielded the V1 boundary location with minimum bias with respect to the measured border. Fig. 2 shows both the signed and unsigned root-mean-squared error between the measured and atlas-predicted boundary over atlas probability threshold. While the error between the V1 boundaries was about 2.5 mm, the average signed boundary distance was just 0.4 ± 0.04 mm, which indicates that the atlas prediction of V1 boundary location has low bias, with a slight tendency to include cortex not actually part of V1 in the prediction. The surface area of measured and predicted V1 is shown for each subject and hemisphere in Table 1.

Comparing the functional and anatomical V1 boundaries

Because the atlas-predicted V1 boundary was found to be highly accurate, it can be used to represent measured anatomical V1 location in our sample of ten *in vivo* subjects. This allows a comparison of the anatomical and functional V1 boundaries. The anatomical boundary was determined via the surface-based probabilistic atlas prediction described above, while the functional boundary was measured using standard fMRI-based visuotopic mapping techniques. The anatomical and functional V1 are shown on an inflated representation of the cortical surface for an example subject in Fig. 3.

The cortical surface-based distance between the functional and anatomical boundary estimates was 2.5 ± 0.05mm on average, which is quite low and identical to the error in the atlas estimate (as determined by comparing to V1 measured from histology). Notably, this error is identical to the voxel-size used in the fMRI scans, which suggests that the error in measuring the V1 boundary is on average the same as a single fMRI voxel. The error for the left hemispheres was

Table 1
The surface area of V1 measured via reconstruction of histological serial section data and estimated by the surface-based probabilistic atlas in the same hemispheres.

Subject	Left hemi		Right hemi	
	Histology	Atlas	Histology	Atlas
1	3295	3509	3127	3146
2	3379	3680	3553	3287
3	2632	3369	2957	3509
4	2865	2847	2583	2564
5	2437	3515	3210	3052
6	2363	2469	1982	1998
7	2479	2613	2294	2103
8	2493	2749	3331	3444
9	2543	3109	2887	2769
10	2505	3214	3363	3460

All surface areas are in mm^2. Subject numbers indicate that the order subjects are shown in Fig. 1 when reading left to right.

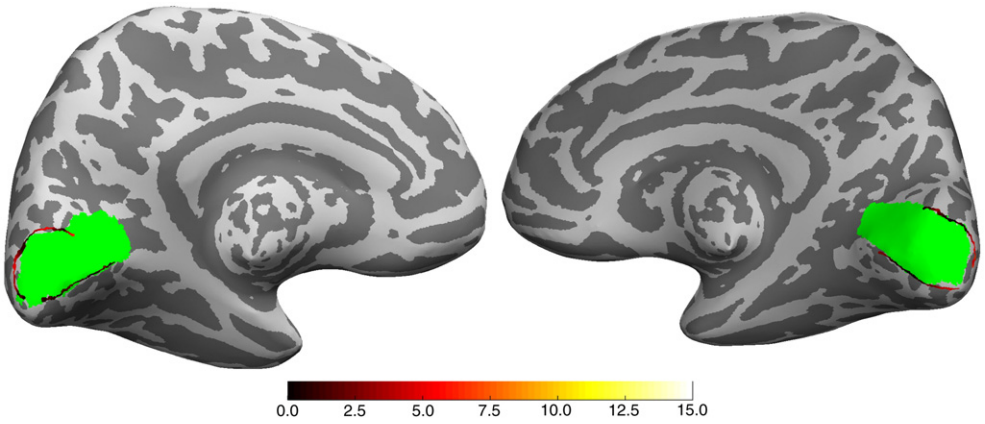

Fig. 3. V1 boundary comparison on the inflated cortex for an example subject. The location of anatomical V1 predicted by the probabilistic atlas is shown in green. Locations determined to lie on the functional V1 boundary via fMRI are colored based on the measured surface-based distance to the nearest location on the anatomical V1 boundary.

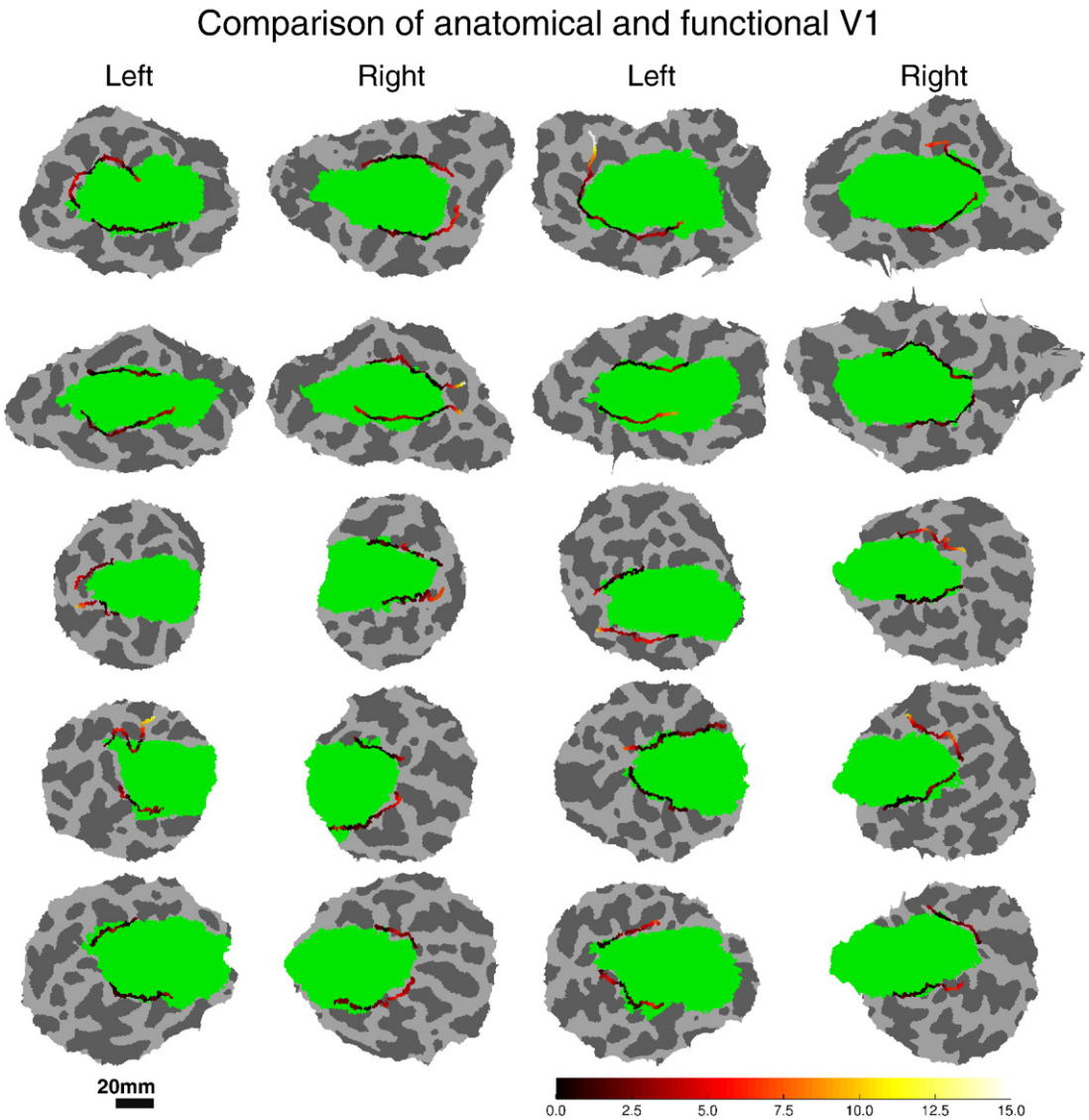

Fig. 4. Alignment of the anatomical and functional V1 boundary. A portion of the flattened left and right occipital lobes is shown for each of the ten subjects with the location of anatomical V1 predicted by the probabilistic atlas shown in green. Locations determined to lie on the functional V1 boundary via fMRI are colored based on the measured surface-based distance to the nearest location on the anatomical V1 boundary. The color bar indicates the measured distance in mm. For each subject the occipital region of each hemisphere is shown with superior to the top and posterior to the left for left hemispheres and to the right for right hemispheres.

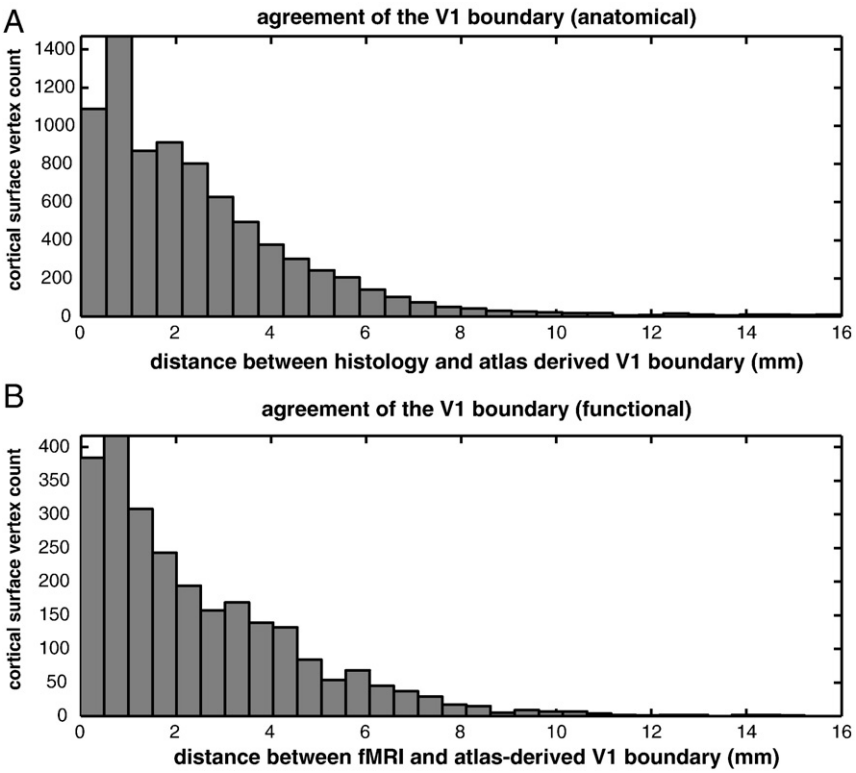

Fig. 5. Agreement between independent measurements of V1 boundary location. (A) A histogram of the distance between the measured V1 boundary defined via analysis of histological data by Amunts et al. (2000) and the predicted V1 boundary based on the atlas of Hinds et al. (2008). The histogram represents the number of surface vertices on the atlas-predicted boundary that fall within a range of distances to the measured boundary. (B) A similar histogram where the distance computed is between each vertex of the functional boundary of V1 and the atlas-predicted boundary in the same subjects.

2.6 ± 0.07 mm and the error for the right hemispheres was 2.5 ± 0.06 mm. Fig. 4 shows a flattened patch of the occipital lobe with both the functional and structural V1 boundaries indicated for each subject. Fig. 5B shows a histogram of the distance between the anatomical and functional boundaries of V1 over all subjects and hemispheres. The number of vertices falls off sharply with increasing discrepancy between the two boundaries, similar to the error between the measured anatomical boundary and the atlas prediction (Fig. 5A).

Discussion

In this work we have demonstrated agreement between two independent methods for defining V1 boundary location in living human subjects. The boundary of functional V1 was measured using standard fMRI-based estimates of visual areas (Sereno et al., 1995; Polimeni et al., 2005), while the boundary of anatomical V1 was predicted using a surface-based probabilistic atlas (Hinds et al., 2008). The atlas prediction was also validated using an independent set of hemispheres where the location of the stria was determined via analysis of histological data (Amunts et al., 2000; Fischl et al., 2008). The agreement of these two boundary measurements up to within the size of one standard fMRI voxel dictates that fMRI scan time can be reduced by replacing functional mapping of V1 location with the probabilistic atlas prediction, which is derived from routinely collected structural MRI scans. Also, this represents the most compelling evidence to date that in human the boundary of the region of cortex containing the stria of Gennari is the same as the region labeled V1 based on its visual topography. Furthermore, that the location of the primary cortical folds is an accurate predictor of functional V1 strongly suggests that the development of the folds is coupled to the mechanisms responsible for determining the location of the visual field representation in cortex (see (Hinds et al., 2008)).

Previous studies of V1 boundaries

The work of Smith (1904), Campbell (1905), Brodmann (1909), Vogt (1911), Flechsig (1920), von Economo and Koskinas (1925), and others establishing differences in the anatomy of the cortical laminae among localized brain regions allowed the correlation of functional representations with specialized anatomy. For V1, such structure/function relationships have been investigated beginning with Inouye (1909) and Holmes (1917) who correlated visual field deficits with the anatomical location of cortical lesions. Little progress beyond these studies has been possible in human subjects due to the difficulty of performing precise mapping of the visual field representation in the same individuals where mapping of microanatomical details is available.

Despite the lack of thorough investigation in human, the relationship between anatomical and functional V1 has been studied in cats by Otsuka and Hassler (1962) and Hubel and Wiesel (1965), who concluded that the location of LGN afferents innervating primary visual cortex (and the colocated stria of Gennari) corresponds precisely to the location of the region identified as functional V1.

If evidence from animal models is taken to demonstrate that anatomical and functional V1 are precisely colocated in human, then previous work investigating the alignment of the anatomical V1 boundary and the primary cortical folds can be used to make statements about the alignment of the visual field representation in V1 and the calcarine sulcus. This connection was made by Smith (1904), who noted that the stria of Gennari corresponded both to the purported location of the visual faculties and was a good predictor of the location of the calcarine sulcus. More quantitative work in this vein was performed by Stensaas et al. (1974) with the goal of deriving an accurate method for targeting electrode placement for visual neuroprostheses based on calcarine sulcus location. Their work (largely corroborated by Rademacher et al., 1993) determined that

the anatomical V1 boundary was well aligned with the calcarine sulcus. On the other hand, Zilles et al. (1997) studied the relationship between area boundaries and sulci and found that V1 does not share a consistent relationship with the sulci. This conclusion was supported by quantitative studies of the intersubject variability of V1 using spatial normalization of cortical geometry in stereotaxic space (Roland et al., 1997; Amunts et al., 2000). These studies suggested that no consistent relationship exists between the representation of the visual field in V1 and the location of the cortical folds.

Recently, the high degree of intersubject variability in V1 location relative to cortical geometry has been revisited by Hinds et al. (2008) and Fischl et al. (2008). These studies demonstrated excellent alignment between V1 and the calcarine sulcus when using surface-based intersubject registration, which provides indirect evidence linking the folds and the visual field representation. However, the results presented here address this question directly. The close agreement between the location of functional V1 and anatomical V1 demonstrated here indicates that the cortical folding pattern of the calcarine sulcus and surrounding regions serves as an accurate predictor of the representation of the vertical meridian of the visual field in V1.

Eliminating V1 functional localizers

Functional localizers are gaining in popularity for fMRI experiments because they can increase power by reducing the number of statistical comparisons and because they can help in the accurate interpretation of the location of brain activation (Saxe et al., 2006). However, functional localizers increase the time required to perform fMRI experiments, especially when they are embedded in factorial designs (Friston et al., 2006).

Functional localizers for visual areas are commonly performed in an auxiliary experiment during the same scanning session as the main experiment. The visual field is often mapped using the same techniques used here to provide a reference for the activations observed in the main experiment. Because we have demonstrated that V1 location estimated from fMRI-based visual field mapping is very similar to the estimate of V1 location provided by the surface-based probabilistic atlas, functional localizer experiments are no longer necessary to locate the V1 boundary. Instead, V1 location can be computed from brain surfaces constructed from a standard T1-weighted structural scan, therefore eliminating the need for extra functional scans. Also, the probabilistic atlas-based method for locating V1 provides an estimate of the entire boundary as opposed to fMRI-based methods, which can only identify about half of the area (see Fig. 4).

MRI of functional and anatomical V1

Two recent studies have investigated the V1 structure/function relationship using MRI in human. Bridge et al. (2005) identified portions of anatomical V1 using high-resolution MRI of the stria of Gennari and functional V1 using fMRI-based mapping of the V1 boundary. The parts of anatomical V1 they were able to identify were nearly always located within functional V1, in agreement with the results presented here. Although Bridge et al. (2005) reported colocation of anatomical and functional V1, their results do not address the correspondence of the V1 boundaries. Quantitative comparison of the V1 boundaries was not possible because they did not have access to a reliable estimate of the anatomical V1 boundary (because the stria of Gennari was not reliably visible due to image acquisition constraints of *in vivo* subjects). Here we have access to a reliable anatomical boundary prediction, which allowed us to quantify boundary alignment.

Wohlschlager et al. (2005) compared anatomical and functional V1 over a population through group atlasing. They used an existing volume-based probabilistic atlas of anatomical V1 derived from histology of ten *ex vivo* brains (Roland et al., 1997; Amunts et al., 2000) to establish the anatomical location of V1 in stereotaxic space. They then created a similar atlas giving the voxel-wise probability of observing functionally defined V1 derived from 12 individuals via fMRI-based visual area mapping. The atlases were then compared, providing a comparison of the variability in stereotaxic space of functional and anatomical V1. Although they reported a good agreement of functional and anatomical V1 at the population level, such comparisons of group-derived atlases cannot address questions regarding the V1 structure/function relationship in individuals. The work presented here measures boundary alignment in individual subjects.

Limitations

Although our findings provide strong evidence that the functional boundary of V1 measured using fMRI corresponds with the anatomical boundary of V1 predicted using a surface-based probabilistic atlas, several sources of error should be considered when interpreting our results. Despite demonstrating that the surface-based atlas prediction of anatomical V1 location exhibits low error on an independent dataset, the atlas prediction is an indirect measurement of anatomical V1 location. A direct measurement of anatomical V1 location would be preferred, but although the stria of Gennari has been imaged *in vivo* (Clark et al., 1992; Barbier et al., 2002; Bridge et al., 2005), no study has demonstrated reliable identification of the stria throughout its entire extent.

As evident in Fig. 1, there is a slight tendency to include cortex not actually in V1 in the atlas prediction. Therefore, locations near the atlas predicted boundary should be considered less reliable than interior portions. An explicit reliability weighting can be considered by examining the vertex-wise probability of lying in V1, which is provided by the atlas. Also, the incomplete range of visual angle which could be stimulated in the MRI scanner limited the anatomical and functional boundary comparison to only about half of V1. Because the regions of V1 that can be measured using fMRI also happen to exhibit lower anatomical variability, the correspondence demonstrated here may not hold for the regions of V1 representing the inner fovea ($<0.5°$) and far periphery ($>40°$).

The gold standard dataset used to validate the probabilistic atlas for anatomical V1 is derived from histological processing and reconstruction of serial brain sections. Its use as a gold standard suggests that we believe this dataset to be more accurate than the high resolution, *ex vivo* MRI scans. In reality there are different errors in these two techniques, dictating that neither is a “gold standard”. Serial section reconstruction is sensitive to slice specific shrinkage due to fixation, physical deformation due to slicing, nonuniform stain intensity between slices, and registration errors both between adjacent slices and of the entire slice dataset to the low-resolution, whole brain MRI scan. The high-resolution *ex vivo* MRI datasets from which the atlas is derived are sensitive to whole-sample shrinkage from fixation, some tissue classification uncertainty due to voxel intensity corruption from MRI noise, geometric distortions from susceptibility inhomogeneity and gradient nonlinearity, and errors in the process of registration to low-resolution, whole brain scans. Because the noise sources in these two methods are largely independent, their close agreement suggests that these noise sources do not substantially affect the location of the V1 boundary. However, future research will focus on whether atlases based on the serial section dataset provide a better atlas of anatomical V1 than the *ex vivo* MRI dataset.

Finally, the effect of changes in brain geometry due to normal development or pathology on V1 registration accuracy has yet to be determined. Until the V1 atlas has been tested on such populations, its use should be limited to healthy adult subjects.

Functional specialization

Demonstrating that the anatomical and functional V1 boundaries are colocated shows that human primary visual cortex contains specialized anatomy (the stria of Gennari) to support a particular functional organization (the topographic map of the visual field), or vice versa. This provides support for the hypothesis that brain function is distributed across the cortex and that regions serving a particular function are specialized anatomically.

An assumption common to many neuroimaging studies is that brain regions supporting particular functions are to some degree consistently located across individuals, and that regions of the cortex showing a distinct microanatomical structure (cortical areas) also exhibit a fairly consistent location. For this reason it is a widespread practice in neuroimaging to refer to cortical areas (or Brodmann areas) when describing the location implicated in a particular function. It remains to be determined whether the specialized microanatomy of cortical areas is directly related to the functional role of corresponding tissue or whether the consistent locations of anatomical and functional regions are unrelated but covarying. The results of this study provide some evidence for the idea that anatomical V1 provides a particular structural arrangement that is necessary for V1 function. In turn, this provides support for the hypothesis that cortical areas are anatomically specialized to support certain brain functions.

References

Amunts, K., Malikovic, A., Mohlberg, H., Schormann, T., Zilles, K., 2000. Brodmann's areas 17 and 18 brought into stereotaxic space-where and how variable? NeuroImage 11 (1), 66–84.

Balasubramanian, M., Polimeni, J.R., and Schwartz, E.L., (In press). Exact geodesics and shortest paths on polyhedral surfaces. *IEEE Trans Pattern Anal Mach Intell.*

Barbier, E., Marrett, S., Danek, A., Vortmeyer, A., van Gelderen, P., Duyn, J., Bandettini, P., Grafman, J., Koretsky, A.P., 2002. Imaging cortical anatomy by high-resolution MR at 3.0 T: detection of the stripe of Gennari in visual area 17. Magn. Reson. Med. 48 (4), 735–738.

Boyd, J. and Matsubara, J., (2005). Repositioning the stria of Gennari [Abstract]. *Abstracts of the Society for Neuroscience.*

Bridge, H., Clare, S., Jenkinson, M., Jezzard, P., Parker, A.J., Matthews, P.M., 2005. Independent anatomical and functional measures of the V1/V2 boundary in human visual cortex. J. Vis. 5 (2), 93–102.

Brodmann, K., (1909). *Vergleichende Lokalisationslehre der Grosshirnrinde in ihren Prinzipien dargestellt auf Grund des Zellenbaues*. J. A. Barth, Leipzig. Translated by Laurence Garey as "Localisation in the Cerebral Cortex" (1994), London: Smith-Gordon, new edition 1999, London: Imperial College Press.

Campbell, A., 1905. Histological Studies on the Localisation of Cerebral Function. Cambridge University Press, London.

Clark, V., Courchesne, E., Grafe, M., 1992. In vivo myeloarchitectonic analysis of human striate and extrastriate cortex using magnetic resonance imaging. Cereb. Cortex 2 (5), 417–424.

Cox, R., Jesmanowicz, A., 1999. Real-time 3D image registration for functional MRI. Magn. Res. Med. 42 (6), 1014–1018.

Dale, A., Sereno, M., 1993. Improved localization of cortical activity by combining EEG and MEG with MRI cortical surface reconstruction: a linear approach. J. Cogn. Neurosci. 5 (2), 162–176.

Dale, A.M., Fischl, B., Sereno, M.I., 1999. Cortical surface-based analysis. segmentation and surface reconstruction. NeuroImage 9 (2), 179–194.

Daniel, P.M., Whitteridge, D., 1961. The representation of the visual field on the cerebral cortex in monkeys. J. Physiol. 159, 203–221.

Duncan, R., Boynton, G., 2003. Cortical magnification within human primary visual cortex correlates with acuity thresholds. Neuron 38 (4), 659–671.

Fischl, B. and Dale, A., (2000). Measuring the thickness of the human cerebral cortex from magnetic resonance images.

Fischl, B., Sereno, M.I., Dale, A.M., 1999a. Cortical surface-based analysis: Inflation, flattening, and a surface-based coordinate system. NeuroImage 9 (2), 195–207.

Fischl, B., Sereno, M.I., Tootell, R.B., Dale, A.M., 1999b. High-resolution intersubject averaging and a coordinate system for the cortical surface. Hum. Brain Mapp. 8 (4), 272–284.

Fischl, B., Liu, A., Dale, A., 2001. Automated manifold surgery: constructing geometrically accurate and topologically correct models of the human cerebral cortex. IEEE Trans. Med. Imaging 20 (1), 70–80.

Fischl, B., Salat, D., Busa, E., Albert, M., Dieterich, M., Haselgrove, C., van der Kouwe, A., Killiany, R., Kennedy, D., Klaveness, S., Montillo, A., Makris, N., Rosen, B., Dale, A., 2002. Whole brain segmentation automated labeling of neuroanatomical structures in the human brain. Neuron 33 (3), 341–355.

Fischl, B., Salat, D., van der Kouwe, A., Makris, N., Segonne, F., Quinn, B., Dale, A., 2004. Sequence-independent segmentation of magnetic resonance images. NeuroImage 23 (Suppl. 1), S69–S84.

Fischl, B., Rajendran, N., Busa, E., Augustinack, J., Hinds, O., Yeo, B., Mohlberg, H., Amunts, K., Zilles, K., 2008. Cortical folding patterns and predicting cytoarchitecture. Cereb. Cortex 18 (8), 1973–1980.

Flechsig, P., 1920. Anatomie des Menschlichen Gehirns und Ruckenmarks auf Myelogenetischer. Thieme, Leipzig.

Friston, K., Rotshtein, P., Geng, J., Sterzer, P., Henson, R., 2006. A critique of functional localisers. NeuroImage 30 (4), 1077–1087.

Hinds, O.P., Rajendran, N., Polimeni, J.R., Augustinack, J.C., Wiggins, G., Wald, L.L., Rosas, H.D., Potthast, A., Schwartz, E.L., Fischl, B., 2008. Accurate prediction of V1 location from cortical folds in a surface coordinate system. NeuroImage 39 (4), 1585–1599.

Holmes, G., 1917. The organization of the visual cortex in man. Br. J. Opthlamol. 2, 353–384.

Hubel, D., Wiesel, T., 1965. Receptive fields and functional architecture in two nonstriate visual areas (18 and 19) of the cat. J. Neurophysiol. 28 (2), 229–289.

Inouye, T., (1909). *Die Sehstörungen bei Schussverletzungen der kortikalen Sehsphäre nach Beobachtungen an Verwundeten der letzten Japanischen Kriege*. W. Engelmann, Leipzig. English translation by M. Glickstein and M. Fahle under the title: *Visual Disturbances following Gunshot Wounds of the Cortical Visual Area*, Brain (Supplement) 123, Oxford University Press, 2000.

Otsuka, R., Hassler, R., 1962. Ueber aufbau und gliederung der corticalen sehsphaere bei der katze. Archiv fuer Psychiatrie und Nervenkrankheiten Vereinigt mit Zeitschrift fuer die Gesamte Neurologie und Psychiatrie 203 (2), 212–234.

Polimeni, J.R., Hinds, O.P., Balasubramanian, M., van der Kouwe, A., Wald, L.L., Dale, A.M., Fischl, B., and Schwartz, E.L., (2005). The human V1–V2–V3 visuotopic map complex measured via fMRI at 3 and 7 Tesla [Abstract]. *Soc Neurosci Abstr.*

Rademacher, J., Caviness, V.S., Steinmetz, H., Galaburda, A.M., 1993. Topographical variation of the human primary cortices: implications for neuroimaging, brain mapping, and neurobiology. Cereb. Cortex 3 (4), 313–329.

Roland, P., Geyer, S., Amunts, K., Schormann, T., Schleicher, A., Malikovic, A., Zilles, K., 1997. Cytoarchitectural maps of the human brain in standard anatomical space. Hum. Brain Mapp. 5 (4), 222–227.

Roland, P.E., Graufelds, C.J., Wacaronhlin, J., Ingelman, L., Andersson, M., Ledberg, A., Pedersen, J., Akerman, S., Dabringhaus, A., Zilles, K., 1994. Human brain atlases for high-resolution functional and anatomical mapping. Hum. Brain Mapp. 1 (3), 173–184.

Saxe, R., Brett, M., Kanwisher, N., 2006. Divide and conquer: a defense of functional localizers. NeuroImage 30 (4), 1088–1096.

Schwartz, E.L., 1977. Spatial mapping in the primate sensory projection: analytic structure and relevance to perception. Biol. Cybern. 25 (4), 181–194.

Sereno, M.I., Dale, A.M., Reppas, J.B., Kwong, K.K., Belliveau, J.W., Brady, T.J., Rosen, B.R., Tootell, R.B., 1995. Borders of multiple visual areas in humans revealed by functional magnetic resonance imaging. Science 268 (5212), 889–893.

Smith, G., 1904. The morphology of the occipital region of the cerebral hemisphere in man and the apes. Anat. Anz. 24, 436–451.

Stensaas, S.S., Eddington, D.K., Dobelle, W.H., 1974. The topography and variability of the primary visual cortex in man. J. Neurosurg. 40 (6), 747–755.

Vogt, O., 1911. Die myeloarchitektonik des isocortex parietalis. J. Psychol. Neurol. 18, 107–118.

von Economo, C., Koskinas, G., 1925. Die Cytoarchitektonik der Hirnrinde des erwachsenen Menschen. Springer, Vienna/Berlin.

Wiggins, G., Triantafyllou, C., Potthast, A., Reykowski, A., Nittka, M., Wald, L., 2006. 32-Channel 3 Tesla receive-only phasedarray head coil with soccer-ball element geometry. MRM 56 (1), 216–223.

Wohlschlager, A.M., Specht, K., Lie, C., Mohlberg, H., Wohlschlager, A., Bente, K., Pietrzyk, U., Stocker, T., Zilles, K., Amunts, K., Fink, G.R., 2005. Linking retinotopic fMRI mapping and anatomical probability maps of human occipital areas V1 and V2. NeuroImage 26 (1), 73–82.

Zilles, K., Schleicher, A., Langemann, C., Amunts, K., Morosan, P., Palomero-Gallagher, N., Schormann, T., Mohlberg, H., Buergel, U., Steinmetz, H., 1997. Quantitative analysis of sulci in the human cerebral cortex: development, regional heterogeneity, gender difference, asymmetry, intersubject variability and cortical architecture. Hum. Brain Mapp. 5 (4), 218–221.